

Optimal Transfer between Elliptic Orbits with Three Tangential Impulses

Andrea Caruso*, Alessandro A. Quarta, Giovanni Mengali

Dipartimento di Ingegneria Civile e Industriale, University of Pisa, I-56122 Pisa, Italy

Abstract

This paper introduces a mathematical model that can be used to evaluate the total velocity variation required to accomplish a given two-dimensional orbit transfer, using up to three tangential impulsive maneuvers. The problem is addressed in an optimal framework, by looking for the transfer trajectory that minimizes the total velocity variation. In particular, by exploiting the nonlinear constraint equations, the total velocity variation can be calculated as a function only of the spacecraft angular position at which the impulses are applied. The small number of control variables involved in the algorithm allows the optimization problem to be solved in a simple and robust way, with a negligible computational effort. The algorithm is able to find the optimal transfer strategy in a generic ellipse-to-ellipse, two-dimensional, mission scenario.

Keywords: Three-impulse two-dimensional transfer, Tangential impulse, Trajectory optimization

Nomenclature

a, b, c	=	auxiliary dimensionless variables, see Eq. (30)
CR	=	crossover ratio
D_i	=	auxiliary function, see Eq. (9)
\det	=	determinant
e	=	eccentricity
\mathbb{F}	=	matrix of coefficients
H	=	Heaviside step function
N	=	number of TIMs/arcs
N_{gen}	=	number of generations
N_i	=	auxiliary function, see Eq. (8)
N_{pop}	=	population size
N_{rev}	=	number of complete revolutions
N_{occ}	=	number of occurrences of a set of genetic algorithm parameters
O	=	primary body center of mass
p	=	semilatus rectum
r	=	primary body-spacecraft distance
$\mathcal{T}(O; r, \theta)$	=	polar reference frame
\mathbf{w}	=	vector of constant terms
\mathbf{x}	=	vector of unknowns
Δv	=	velocity variation
δ	=	grid search step

*Corresponding author

Email addresses: andrea.caruso@ing.unipi.it (Andrea Caruso), a.quarta@ing.unipi.it (Alessandro A. Quarta), g.mengali@ing.unipi.it (Giovanni Mengali)

η	=	variation of specific angular momentum
θ	=	polar angle
θ_{ij}	=	angular difference ($\theta_j - \theta_i$)
μ	=	gravitational parameter
ν	=	true anomaly
ω	=	longitude of pericenter

Subscripts

0	=	initial, parking orbit
f	=	final, target orbit
i	=	i th TIM/arc
tot	=	total

Accent

\sim	=	dimensionless quantity
--------	---	------------------------

Acronyms

TIM	=	tangential impulsive maneuver
-----	---	-------------------------------

1. Introduction

The study of a multi-impulse transfer between two coplanar and Keplerian orbits is a classical problem of astrodynamics [1, 2], which is usually analyzed within an optimal framework by looking for the transfer trajectory that minimizes the propellant consumption, the total flight time, or a suitable combination of these two quantities [3, 4, 5].

A particular, yet important case, is when the orbit transfer is obtained with a set of tangential impulsive maneuvers (TIMs), which change the magnitude of the spacecraft velocity vector without affecting its direction. Indeed, Hohmann, bi-elliptic, or bi-parabolic transfers represent just a particular optimal multi-TIM case in which the parking and target orbits are both circular. The multi-TIM transfer has received growing attention in the recent literature [6, 7]. For example, [8] calculated the total velocity variation for two-TIMs from a geometrical perspective, while [9] discussed the existence conditions for a solution to a two-TIM transfer, and [10] developed a model for studying the transfer from a elliptic parking orbit toward a hyperbolic target orbit with a given excess velocity vector, using either a single TIM, or a multi-TIM approach. More recently, [11] developed a mathematical model to determine the global minimum velocity variation for a cotangential transfer, using a graphical method that uses a linear systems approach for multi-TIM trajectory analysis [12].

The aim of this paper is to introduce a mathematical model that, starting from the approach by [11], is able to obtain an accurate approximation of the (global) minimum total velocity variation required to complete a three-TIM transfer between two coplanar, Keplerian, orbits. In this sense, this paper extends the recent literature results [11] to a more complex mission scenario and also reveals the existence of interesting singular cases that are absent in the classical cotangential transfer. In particular, the proposed procedure gives both the minimum velocity variation, and the position of the three (optimal) impulsive maneuvers, which can be used as an initial guess into a numerical optimization algorithm to obtain a refined solution with a small computational effort.

The remainder of this paper is organized as follows. Section 2 gives a description of the problem, whereas Section 3 introduces the mathematical model used to compute the total velocity change as a function of the control variables. Section 4 describes the optimization procedure, while section 5 presents some mission applications. Finally, the last section contains some concluding remarks.

2. Problem description

Consider a spacecraft in a Keplerian elliptic orbit of eccentricity $e_0 < 1$ and semilatus rectum p_0 , which moves around a primary body of gravitational parameter μ . Introduce a polar reference frame $\mathcal{T}(O; r, \theta)$ with origin O at the primary body center-of-mass, where r is the primary body-spacecraft distance, and θ is the polar angle measured counterclockwise from the parking orbit apse line (that is, O -pericenter direction); see Fig. 1. In the special case of circular parking orbit ($e_0 = 0$), the polar angle θ is measured counterclockwise from a fixed direction. The problem is to calculate the minimum total velocity variation Δv_{tot} required to transfer the spacecraft to a coplanar, Keplerian, target orbit of eccentricity e_f , semilatus rectum p_f , and longitude of the pericenter $\omega_f \in [0, 2\pi)$ rad, using three TIMs. In particular, ω_f is the angle (measured counterclockwise) from the parking orbit to the target orbit apse line (primary body-pericenter direction). In the special case of circular target orbit ($e_f = 0$), the longitude of the pericenter is set equal to zero, that is, $\omega_f = 0$ rad.

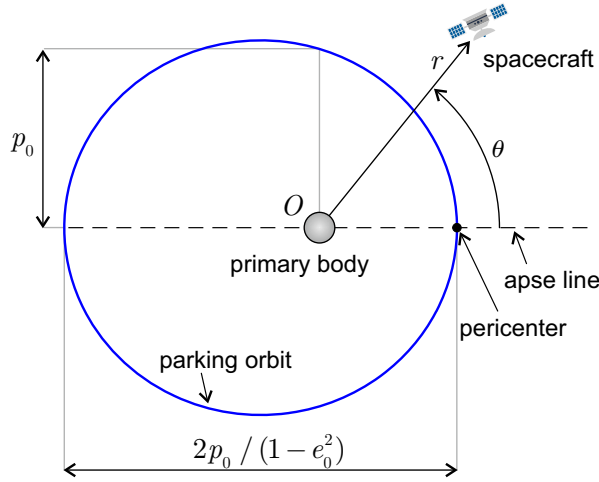


Figure 1: Reference frame and parking orbit characteristics.

The spacecraft transfer trajectory and the velocity variation of each TIM can be analyzed with the model proposed by [12], which is now briefly summarized in the general case in which the spacecraft performs $N \in \mathbb{N}$ TIMs. Assume a Keplerian motion between two successive maneuvers, that is, the orbital perturbations between two successive TIMs are neglected. The whole spacecraft trajectory can be divided into N conic arcs, each one starting at the point where the tangential impulse is applied; see Fig. 2.

The generic (i th) arc is characterized by a set of three orbital parameters $\{e_i, p_i, \omega_i\}$, with $i = 1, 2, \dots, N$. Note that the triplet $\{e_N, p_N, \omega_N\}$ defines the characteristics of the spacecraft orbit after the last (N th) TIM. Let θ_i be the polar angle at which the i th TIM occurs, with $\theta_1 \in [0, 2\pi)$ rad and

$$\theta_1 < \theta_2 < \dots < \theta_N \quad (1)$$

and introduce the dimensionless (positive) parameter

$$\eta_i \triangleq \sqrt{\frac{p_i}{p_{i-1}}} \quad \text{with} \quad i = 1, 2, \dots, N \quad (2)$$

In particular, $\eta_i > 0$ quantifies the variation of the specific angular momentum due to the i th TIM since, by definition, $\eta_i \equiv h_i/h_{i-1}$, where h_i (or h_{i-1}) is the specific angular momentum just after (or just before) the i th impulsive maneuver. The spacecraft true anomaly ν_0 (or ν_f) on the parking (or target) orbit at the beginning (or end) of the transfer can be written as a function of polar angle θ_1 (or θ_N) as

$$\nu_0 = \theta_1 \quad , \quad \nu_f = \theta_N - \omega_f - 2\pi \left\lfloor \frac{\theta_N - \omega_f}{2\pi} \right\rfloor \quad (3)$$

The polar equation $r = r(\theta)$ (with $\theta \in [\theta_1, \theta_N]$) of the spacecraft transfer trajectory reduces to

$$r(\theta) = \frac{p_0}{1 + e_0 \cos \theta + \sum_{k=1}^N \frac{1 - \eta_k^2}{\prod_{j=1}^k \eta_j^2} [1 - \cos(\theta - \theta_k)] H(\theta - \theta_k)} \quad (10)$$

where $H(\square)$ is the Heaviside step function, defined as

$$H(\theta - \theta_k) = \begin{cases} 0 & \text{if } \theta \leq \theta_k \\ 1 & \text{if } \theta > \theta_k \end{cases} \quad (11)$$

The velocity variation Δv_i of the i th maneuver can be written as [12]

$$\Delta v_i = |\eta_i - 1| \sqrt{\frac{2\mu}{r_i} - \frac{\mu(1 - e_{i-1}^2)}{p_{i-1}}} \quad (12)$$

where $r_i \triangleq r(\theta_i)$ is the O -spacecraft distance at the generic i th TIM with

$$r_i = \frac{p_0}{1 + e_0 \cos \theta_i + \sum_{k=1}^N \frac{1 - \eta_k^2}{\prod_{j=1}^k \eta_j^2} [1 - \cos(\theta_i - \theta_k)] H(\theta_i - \theta_k)} \quad (13)$$

The total velocity variation Δv_{tot} is therefore given by

$$\Delta v_{\text{tot}} = \sum_{i=1}^N \Delta v_i \equiv \sum_{i=1}^N |\eta_i - 1| \sqrt{\frac{2\mu}{r_i} - \frac{\mu(1 - e_{i-1}^2)}{p_{i-1}}} \quad (14)$$

which can be rewritten in a more useful dimensionless form, independent of the gravitational parameter μ , as

$$\Delta \tilde{v}_{\text{tot}} \triangleq \frac{\Delta v_{\text{tot}}}{\sqrt{\mu/p_0}} = \sum_{i=1}^N |\eta_i - 1| \sqrt{\frac{2p_0}{r_i} - \frac{p_0(1 - e_{i-1}^2)}{p_{i-1}}} \quad (15)$$

Note that if $\eta_i = 1$, the corresponding value of Δv_i is zero, that is, the i th maneuver does not take place.

The problem is to define a general procedure that allows $\Delta \tilde{v}_{\text{tot}}$ to be minimized. In the special case when $N = 2$, [11] have recently developed a general, graphical, method that can be used to calculate the minimum velocity variation necessary to accomplish a general orbit-to-orbit, two-dimensional, transfer. The next section presents a new method that extends the analytical results of [11] to the important case of a two-dimensional transfer with a maximum number of three TIMs.

3. Transfer case with three-TIMs

Consider now a transfer with $N = 3$ tangential impulses, in which the spacecraft transfer trajectory consists of two conic arcs. A conceptual sketch of the transfer is shown in Fig. 3, where θ_{12} (or θ_{23}) is the polar angle swept by the spacecraft between the first and second (or second and third) TIM. Because the two arcs are Keplerian, the following constraints are introduced

$$\theta_{12} \in (0, 2\pi) \text{ rad} \quad , \quad \theta_{23} \in (0, 2\pi) \text{ rad} \quad (16)$$

that is, the angle swept out by the spacecraft within two consecutive maneuvers is less than a full revolution around the primary body. Note that the limiting case when either θ_{12} or θ_{23} goes to zero corresponds to a two-impulse transfer, while the case when $\theta_{12} = \theta_{23} \rightarrow 0$ refers to a single-impulse transfer.

Bearing in mind Eq. (3) and the scheme of Fig. 3, the angular position of the three TIMs can be written as a function of $\{\nu_0, \theta_{12}, \theta_{23}\}$ as

$$\theta_1 = \nu_0 \quad , \quad \theta_2 = \nu_0 + \theta_{12} \quad , \quad \theta_3 = \nu_0 + \theta_{12} + \theta_{23} \quad (17)$$

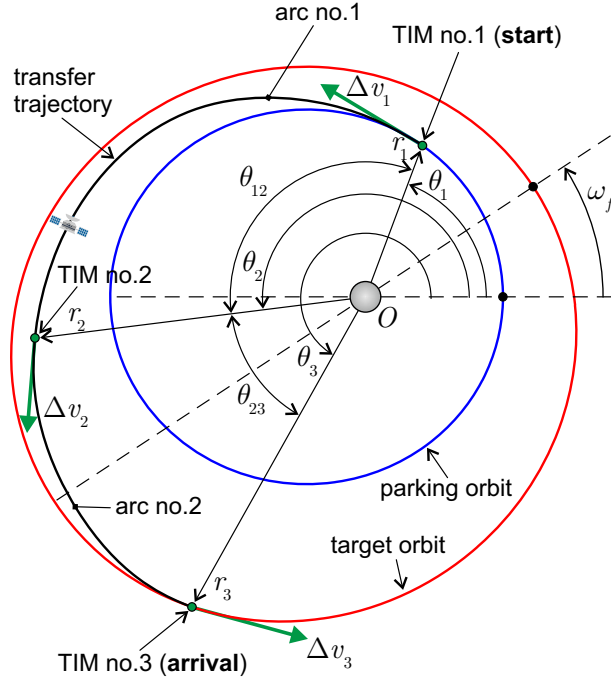


Figure 3: Schematic representation of a three-impulse, two-dimensional, orbit transfer between two (generic) elliptic orbits.

From Eqs. (4) and (17), the number of complete revolutions during the transfer is

$$N_{\text{rev}} = \left\lfloor \frac{\theta_{12} + \theta_{23}}{2\pi} \right\rfloor \in \{0, 1\} \quad (18)$$

Substituting Eqs. (5)–(6) and (13) into Eq. (12), the velocity variations in the three TIMs can be written as a function of $\{\theta_1, \theta_2, \theta_3, \eta_1, \eta_2, \eta_3\}$ as

$$\Delta v_1 = |\eta_1 - 1| \sqrt{\frac{\mu}{p_0}} \sqrt{e_0^2 + 2e_0 \cos \theta_1 + 1} \quad (19)$$

$$\begin{aligned} \Delta v_2 = |\eta_2 - 1| \sqrt{\frac{\mu}{p_0}} \left\{ \eta_1^2 (e_0^2 + 2e_0 \cos \theta_1 + 1) + \right. \\ \left. + 2e_0 (\cos \theta_2 - \cos \theta_1) + 2(1/\eta_1^2 - 1)[1 - \cos(\theta_2 - \theta_1)] \right\}^{1/2} \end{aligned} \quad (20)$$

$$\begin{aligned} \Delta v_3 = |\eta_3 - 1| \sqrt{\frac{\mu}{p_0}} \left\{ 2 \left[1 + e_0 \cos \theta_3 + \frac{1 - \eta_1^2}{\eta_1^2} [1 - \cos(\theta_3 - \theta_1)] + \right. \right. \\ \left. \left. + \frac{1 - \eta_2^2}{\eta_1^2 \eta_2^2} [1 - \cos(\theta_3 - \theta_2)] \right] - \frac{1}{\eta_1^2 \eta_2^2} + \eta_1^2 \eta_2^2 (N_2^2 + D_2^2) \right\}^{1/2} \end{aligned} \quad (21)$$

where, according to Eqs. (8)–(9), N_2 and D_2 are given by

$$N_2 = \frac{1 - \eta_1^2}{\eta_1^2} \sin \theta_1 + \frac{1 - \eta_2^2}{\eta_1^2 \eta_2^2} \sin \theta_2 \quad (22)$$

$$D_2 = e_0 - \frac{1 - \eta_1^2}{\eta_1^2} \cos \theta_1 - \frac{1 - \eta_2^2}{\eta_1^2 \eta_2^2} \cos \theta_2 \quad (23)$$

From Eq. (15), in this case the (dimensionless) total velocity variation to be minimized is

$$\Delta \tilde{v}_{\text{tot}} = \frac{\Delta v_1 + \Delta v_2 + \Delta v_3}{\sqrt{\mu/p_0}} \quad (24)$$

where $\{\Delta v_1, \Delta v_2, \Delta v_3\}$ are given by Eqs. (19)–(21). Note that $\Delta \tilde{v}_{\text{tot}}$ is, in general, an involved function of $\{\theta_1, \theta_2, \theta_3, \eta_1, \eta_2, \eta_3\}$. However, the values of θ_i and η_i are not all independent variables. In fact, because the spacecraft must be inserted into a target orbit with given values of $\{p_f, e_f, \omega_f\}$, from Eqs. (5)–(7) the boundary constraints to be met after the third (and last) TIM, are

$$p_f \equiv \eta_1^2 \eta_2^2 \eta_3^2 p_0 \quad (25)$$

$$e_f \equiv \eta_1^2 \eta_2^2 \eta_3^2 \sqrt{N_3^2 + D_3^2} \quad (26)$$

$$\sin \omega_f \equiv -\frac{N_3}{\sqrt{N_3^2 + D_3^2}} \quad , \quad \cos \omega_f \equiv \frac{D_3}{\sqrt{N_3^2 + D_3^2}} \quad (27)$$

Also, according to Eqs. (8)–(9), the auxiliary functions N_3 and D_3 are

$$N_3 = \frac{1 - \eta_1^2}{\eta_1^2} \sin \theta_1 + \frac{1 - \eta_2^2}{\eta_1^2 \eta_2^2} \sin \theta_2 + \frac{1 - \eta_3^2}{\eta_1^2 \eta_2^2 \eta_3^2} \sin \theta_3 \quad (28)$$

$$D_3 = e_0 - \frac{1 - \eta_1^2}{\eta_1^2} \cos \theta_1 - \frac{1 - \eta_2^2}{\eta_1^2 \eta_2^2} \cos \theta_2 - \frac{1 - \eta_3^2}{\eta_1^2 \eta_2^2 \eta_3^2} \cos \theta_3 \quad (29)$$

Equations (25)–(27) may be rearranged to obtain the triplet $\{\eta_1, \eta_2, \eta_3\}$ as a function of $\{\theta_1, \theta_2, \theta_3\}$ (or $\{\nu_0, \theta_{12}, \theta_{23}\}$, see Eqs. (17)). To that end, we introduce the dimensionless variables $\{a, b, c\}$ defined as

$$a \triangleq \frac{1 - \eta_1^2}{\eta_1^2} \quad , \quad b \triangleq \frac{1 - \eta_2^2}{\eta_1^2 \eta_2^2} \quad , \quad c \triangleq \frac{1 - \eta_3^2}{\eta_1^2 \eta_2^2 \eta_3^2} \quad (30)$$

from which, bearing in mind Eq. (25), it may be verified that

$$a + b + c = \frac{1 - \eta_1^2 \eta_2^2 \eta_3^2}{\eta_1^2 \eta_2^2 \eta_3^2} \equiv \frac{p_0}{p_f} - 1 \quad (31)$$

Note that $\{\eta_1^2, \eta_2^2, \eta_3^2\}$ can be obtained from $\{a, b, c\}$ through the following equations

$$\eta_1^2 = \frac{1}{1 + a} \quad , \quad \eta_2^2 = \frac{1 + a}{1 + a + b} \quad , \quad \eta_3^2 = \frac{1 + a + b}{1 + a + b + c} \quad (32)$$

In addition, using Eqs. (25)–(27), N_3 and D_3 can be written as a function of the characteristics of the parking and target orbit as

$$N_3 = -e_f (p_0/p_f) \sin \omega_f \quad , \quad D_3 = e_f (p_0/p_f) \cos \omega_f \quad (33)$$

Therefore, substituting Eqs. (30) and (33) into Eqs. (28)–(29), and combining the latter with Eq. (31), the resultant system of linear equations may be written in matrix form as

$$\mathbb{F} \mathbf{x} = \mathbf{w} \quad (34)$$

where

$$\mathbb{F} \triangleq \begin{bmatrix} \sin \theta_1 & \sin \theta_2 & \sin \theta_3 \\ \cos \theta_1 & \cos \theta_2 & \cos \theta_3 \\ 1 & 1 & 1 \end{bmatrix} \quad , \quad \mathbf{x} \triangleq \begin{bmatrix} a \\ b \\ c \end{bmatrix} \quad , \quad \mathbf{w} \triangleq \begin{bmatrix} -e_f (p_0/p_f) \sin \omega_f \\ e_0 - e_f (p_0/p_f) \cos \omega_f \\ (p_0/p_f) - 1 \end{bmatrix} \quad (35)$$

Clearly, a single solution exists for Eq. (34) only if \mathbb{F} is nonsingular. Since

$$\det \mathbb{F} = \sin(\theta_{12} + \theta_{23}) - \sin \theta_{12} - \sin \theta_{23} \quad (36)$$

the matrix \mathbb{F} is singular (i.e., $\det \mathbb{F} = 0$) when $\theta_{12} + \theta_{23} = 2\pi$ rad, that is, when $\theta_3 - \theta_1 = 2\pi$ rad. The case in which $\det \mathbb{F} = 0$ is involved and requires a separate discussion; see the Appendix. To simplify the analysis, it is now assumed that $\det \mathbb{F} \neq 0$, that is, $\theta_3 - \theta_1 \neq 2\pi$ rad. In that case, the triplet $\{a, b, c\}$ is found from Eq. (34) as

$$a = \frac{(1 - p_0/p_f) \sin(\theta_3 - \theta_2) + e_0(\sin \theta_3 - \sin \theta_2) + e_f(p_0/p_f)[\sin(\omega_f - \theta_3) - \sin(\omega_f - \theta_2)]}{\sin(\theta_3 - \theta_1) - \sin(\theta_2 - \theta_1) - \sin(\theta_3 - \theta_2)} \quad (37)$$

$$b = \frac{(1 - p_0/p_f) \sin(\theta_1 - \theta_3) + e_0(\sin \theta_1 - \sin \theta_3) + e_f(p_0/p_f)[\sin(\omega_f - \theta_1) - \sin(\omega_f - \theta_3)]}{\sin(\theta_3 - \theta_1) - \sin(\theta_2 - \theta_1) - \sin(\theta_3 - \theta_2)} \quad (38)$$

$$c = \frac{(1 - p_0/p_f) \sin(\theta_2 - \theta_1) + e_0(\sin \theta_2 - \sin \theta_1) + e_f(p_0/p_f)[\sin(\omega_f - \theta_2) - \sin(\omega_f - \theta_1)]}{\sin(\theta_3 - \theta_1) - \sin(\theta_2 - \theta_1) - \sin(\theta_3 - \theta_2)} \quad (39)$$

Note the symmetry of the results, that is, each numerator of $\{a, b, c\}$ is obtained from the preceding one by cyclic permutation of indexes in θ_i . Finally, from Eqs. (32), it is found that

$$\eta_1^2 = \frac{(p_f/p_0) [\sin(\theta_2 - \theta_1) + \sin(\theta_3 - \theta_2) - \sin(\theta_3 - \theta_1)]}{d_1} \quad (40)$$

$$\eta_2^2 = \frac{(p_f/p_0) (\sin \theta_2 - \sin \theta_3)}{d_2} \quad (41)$$

$$\eta_3^2 = \frac{p_f/p_0}{\eta_1^2 \eta_2^2} \quad (42)$$

where

$$d_1 \triangleq \sin(\theta_3 - \theta_2) + e_f [\sin(\omega_f - \theta_3) - \sin(\omega_f - \theta_2)] + (p_f/p_0) \{\sin(\theta_2 - \theta_1) - \sin(\theta_3 - \theta_1) + e_0 [\sin \theta_3 - \sin \theta_2]\} \quad (43)$$

$$d_2 \triangleq (p_f/p_0) [\sin \theta_2 - \sin \theta_1] - \eta_1^2 \sin \theta_3 + \eta_1^2 (p_f/p_0) \sin \theta_1 - e_f \eta_1^2 \sin \omega_f \quad (44)$$

In general, for a given triplet $\{\theta_1, \theta_2, \theta_3\}$, negative values of η_1^2 or η_2^2 may occur; see the right hand side of Eqs. (40) and (41). Those triplets of θ_i correspond however to infeasible transfers, as thoroughly discussed by [11] in the simplified case of two-TIMs, and must be discarded in the optimization process.

As a result, as long as $\theta_3 \neq \theta_1 + 2\pi$ rad, from Eqs. (19)–(21) and (24) the total velocity variation is a function of three independent variables, that is, $\Delta \tilde{v}_{\text{tot}} = \Delta \tilde{v}_{\text{tot}}(\theta_1, \theta_2, \theta_3)$, because η_1 , η_2 , and η_3 are given by Eqs. (40)–(42). The optimal transfer with three TIMs is obtained by choosing the triplet $\{\theta_1, \theta_2, \theta_3\}$ that minimizes $\Delta \tilde{v}_{\text{tot}}$ in Eq. (24). A more detailed description of the procedure used to solve the optimization problem is given in the next section.

4. Trajectory optimization procedure

For a parking and target orbit of given characteristics $\{p_0, e_0, p_f, e_f, \omega_f\}$, the problem consists in calculating the minimum velocity variation Δv_{tot} required by the three-TIM transfer. From the previous discussion, that amounts to minimizing the value of $\Delta \tilde{v}_{\text{tot}}$ given by Eq. (24) as a function of the three polar angles $\{\theta_1, \theta_2, \theta_3\}$. The search space is usually characterized by many local minima, and so the calculation of the minimum $\Delta \tilde{v}_{\text{tot}}$ requires an accurate initial guess of $\{\theta_1, \theta_2, \theta_3\}$. To this end, the equations obtained in the

previous section can be used to implement an efficient grid search algorithm using the following procedure. 1) The search space $\nu_0 \in [0, 2\pi)$ rad, $\theta_{12} \in (0, 2\pi)$ rad, $\theta_{23} \in (0, 2\pi)$ rad (with $\theta_{12} + \theta_{23} \neq 2\pi$), is first arranged in a grid of data, with a step size δ , which are used to generate a set of candidate triplets; 2) the polar angles $\{\theta_1, \theta_2, \theta_3\}$ are calculated from Eqs. (17) as a function of $\{\nu_0, \theta_{12}, \theta_{13}\}$; 3) the value of each η_i^2 is obtained from Eqs. (40)–(42) by discharging the triplets $\{\nu_0, \theta_{12}, \theta_{23}\}$ that generate $\eta_i^2 < 0$; 4) the value of the generic velocity variation Δv_i is calculated from Eqs. (19)–(21) while the value of $\Delta \tilde{v}_{\text{tot}}$ is obtained from Eq. (24); 5) the whole function's domain is divided into a set of sub-domains, and the minimum of the three-dimensional array $\Delta \tilde{v}_{\text{tot}} = \Delta \tilde{v}_{\text{tot}}(\nu_0, \theta_{12}, \theta_{23})$ (along with the corresponding polar angles θ_i) is evaluated inside each of the sub-domains using a sorting procedure; 6) the guess solutions found inside each sub-domain are then refined with a local minimizer such as, for example, the simplex algorithm, [13] implemented in MATLAB's built-in function `fminsearch`; 7) the global minimum is chosen as the solution with the lowest $\Delta \tilde{v}_{\text{tot}}$ among those obtained with this procedure. The local minimizer is run starting from different initial guess points to better explore the search domain and avoid possible local minima. Steps 1-7 are then repeated with a thicker grid until the solution does not change within a given tolerance limit. All of the simulations in this paper have been carried out on a personal computer with an Intel processor Core i7-7500U CPU at 2.70 GHz and with 8.00 GB of RAM.

The proposed approach has been validated in different test cases with a global optimization procedure that uses a genetic algorithm to find the optimal value of the triplet $\{\theta_1, \theta_2, \theta_3\}$. MATLAB's built-in function `ga` has been used in this work. The genetic-based algorithm starts by randomly generating a population of candidate solutions. For each member of the population, the cost function (that is, $\Delta \tilde{v}_{\text{tot}}$) is evaluated using the previous mathematical model. The members of the population with the best fitness values are more likely to be selected to produce a new generation of possible solutions using the crossover and mutation operators. The initial population of the genetic algorithm is generated using the option 'gacreationlinearfeasible', which creates a population that satisfies the bounds and linear constraints. At each generation, the best individuals are chosen using the 'selectiontournament' option, while 'mutationadaptfeasible' and 'crossoverintermediate' are used for mutation and crossover operators, respectively (these are the default options for optimization problems with linear constraints). Some parameters must be tuned to obtain a good performance of the optimization method in terms of its effectiveness and computational cost. These parameters are the population size N_{pop} , the number of generations N_{gen} and the crossover ratio CR . In particular, the following values were chosen for the numerical simulations: $N_{\text{pop}} = \{20, 50, 100, 150\}$, $N_{\text{gen}} = \{20, 50, 100\}$, and $CR = \{0.2, 0.5, 0.8\}$. For each combination of those values, $N_e = 100$ runs of the genetic algorithm have been simulated, and the average value and standard deviation for each population of results have been computed. An example is shown in Tab. 1, which refers to a transfer with $p_f/p_0 = 2$, $e_0 = 0.85$, $e_f = 0.9$ and $\omega_f = 15$ deg.

The last column of Tab. 1 reports the computational time required by 100 runs of the genetic algorithm-based procedure. The results also include the computational time required by the algorithm to generate an initial feasible population¹, which satisfies the conditions of Eq. (1) and (16).

Using the data in Tab. 1, the 36 combinations of parameters $\{N_{\text{pop}}, N_{\text{gen}}, CR\}$ have all been compared. A Student's t-test was applied to check the existence of a possible statistically significant deviation between the results. In the absence of a marked difference between two populations, the combination requiring less computational effort is selected, otherwise that with the smallest mean value is chosen. The best solution corresponds to the combination with the highest value of N_{occ} . Tab. 2 shows the result of the t-test, from which the parameters to be used are a population size of 100 members, a number of generations equal to 20 and a crossover ratio equal to 0.2.

5. Mission scenarios and numerical simulations

The proposed approach is now applied to some mission scenarios to find the transfer trajectory that requires the minimum velocity variation using a maximum number of three TIMs. In particular, a circle-to-circle problem and a more general ellipse-to-ellipse transfer are discussed.

¹See the website [retrieved in April 2, 2019]: <https://it.mathworks.com/help/gads/genetic-algorithm-options.html#f14223>

N_{pop}	N_{gen}	CR	Best solution	Mean value	Std. deviation	Comp. time (s)
20	20	0.2	0.11880017	0.12083893	0.00284452	28.8
		0.5	0.11880143	0.12082688	0.00276228	29.6
		0.8	0.11883908	0.12125160	0.00254819	28.6
	50	0.2	0.11879996	0.12020482	0.00167190	47.2
		0.5	0.11879996	0.12050435	0.00218423	46.8
		0.8	0.11880036	0.12090092	0.00306457	46.1
	100	0.2	0.11879996	0.12029709	0.00173641	75.7
		0.5	0.11879996	0.12018277	0.00139449	76.7
		0.8	0.11880003	0.12102916	0.00269748	74.5
50	20	0.2	0.11880006	0.11969893	0.00064848	75.4
		0.5	0.11880016	0.11990915	0.00070161	76.1
		0.8	0.11879996	0.11981625	0.00065469	73.4
	50	0.2	0.11879996	0.11971109	0.00063986	101.7
		0.5	0.11879996	0.11962524	0.00064724	98.6
		0.8	0.11879996	0.11980578	0.00080453	96.0
	100	0.2	0.11879996	0.11963880	0.00066012	147.3
		0.5	0.11879996	0.11966463	0.00067343	141.3
		0.8	0.11879996	0.11982309	0.00067615	135.9
100	20	0.2	0.11879996	0.11942641	0.00066536	307.6
		0.5	0.11879996	0.11950118	0.00065972	304.5
		0.8	0.11879996	0.11954838	0.00066344	303.6
	50	0.2	0.11879996	0.11944728	0.00067658	351.4
		0.5	0.11879996	0.11943034	0.00065928	350.7
		0.8	0.11879996	0.11953773	0.00066867	346.7
	100	0.2	0.11879996	0.11932544	0.00066056	422.0
		0.5	0.11879996	0.11937319	0.00066727	407.7
		0.8	0.11879996	0.11948118	0.00066469	397.6
150	20	0.2	0.11879996	0.11936678	0.00065052	1101.5
		0.5	0.11879996	0.11937167	0.00065309	1093.4
		0.8	0.11879996	0.11952432	0.00068116	1104.6
	50	0.2	0.11879996	0.11924408	0.00063596	1143.9
		0.5	0.11879996	0.11924680	0.00063353	1135.4
		0.8	0.11879996	0.11936913	0.00065433	1135.9
	100	0.2	0.11879996	0.11923088	0.00063139	1222.1
		0.5	0.11879996	0.11932566	0.00065725	1198.2
		0.8	0.11879996	0.11943192	0.00066069	1201.8

Table 1: Best solution, mean value, standard deviation and computational time of $N_e = 100$ runs of genetic algorithm using different combinations of N_{pop} , N_{gen} and CR , for a transfer with $p_f/p_0 = 2$, $e_0 = 0.85$, $e_f = 0.9$, and $\omega_f = 15$ deg.

$\{N_{\text{pop}}, N_{\text{gen}}, CR\}$	N_{occ}	$\{N_{\text{pop}}, N_{\text{gen}}, CR\}$	N_{occ}
$\{20, 20, 0.2\}$	6	$\{100, 20, 0.2\}$	31
$\{20, 20, 0.5\}$	5	$\{100, 20, 0.5\}$	28
$\{20, 20, 0.8\}$	4	$\{100, 20, 0.8\}$	25
$\{20, 50, 0.2\}$	6	$\{100, 50, 0.2\}$	26
$\{20, 50, 0.5\}$	5	$\{100, 50, 0.5\}$	28
$\{20, 50, 0.8\}$	3	$\{100, 50, 0.8\}$	22
$\{20, 100, 0.2\}$	3	$\{100, 100, 0.2\}$	29
$\{20, 100, 0.5\}$	5	$\{100, 100, 0.5\}$	28
$\{20, 100, 0.8\}$	0	$\{100, 100, 0.8\}$	23
$\{50, 20, 0.2\}$	19	$\{150, 20, 0.2\}$	25
$\{50, 20, 0.5\}$	10	$\{150, 20, 0.5\}$	26
$\{50, 20, 0.8\}$	16	$\{150, 20, 0.8\}$	16
$\{50, 50, 0.2\}$	15	$\{150, 50, 0.2\}$	29
$\{50, 50, 0.5\}$	21	$\{150, 50, 0.5\}$	30
$\{50, 50, 0.8\}$	14	$\{150, 50, 0.8\}$	22
$\{50, 100, 0.2\}$	15	$\{150, 100, 0.2\}$	27
$\{50, 100, 0.5\}$	16	$\{150, 100, 0.5\}$	23
$\{50, 100, 0.8\}$	11	$\{150, 100, 0.8\}$	18

Table 2: Number of occurrences N_{occ} of a set of genetic algorithm parameters.

5.1. Circle-to-circle transfer

A circle-to-circle transfer, in which $e_0 = e_f = 0$ and $p_f > p_0$, is first discussed for validation purposes. In fact, the globally optimal solution is known to be the Hohmann transfer when $p_f/p_0 < 11.94$, otherwise the optimal transfer is a bi-parabolic trajectory. Note that the Hohmann transfer may be thought of as the optimal three TIM-transfer in which one of η_i is equal to 1, while the bi-parabolic transfer coincides with the optimal three TIM-transfer with $\Delta v_2 = 0$.

Without loss of generality, the first TIM is assumed to occur at $\theta_1 = 0$, while ω_f is set equal to zero. In that case, Eqs. (40)–(42) reduce to

$$\eta_1^2 = \frac{(p_f/p_0) [\sin(\theta_2 - \theta_3) - \sin \theta_2 + \sin \theta_3]}{\sin(\theta_2 - \theta_3) + (p_f/p_0) (\sin \theta_3 - \sin \theta_2)} \quad (45)$$

$$\eta_2^2 = \frac{\sin(\theta_2 - \theta_3) + (p_f/p_0) (\sin \theta_3 - \sin \theta_2)}{\sin(\theta_2 - \theta_3) + \sin \theta_3 - (p_f/p_0) \sin \theta_2} \quad (46)$$

$$\eta_3^2 = \frac{\sin(\theta_2 - \theta_3) + \sin \theta_3 - (p_f/p_0) \sin \theta_2}{\sin(\theta_2 - \theta_3) - \sin \theta_2 + \sin \theta_3} \quad (47)$$

which, from the previous analysis, are valid as long as $\det \mathbb{F} \neq 0$, that is, $\theta_3 \neq 2\pi$. For a given value of the ratio $p_f/p_0 \neq 1$, the triplet $\{\eta_1^2, \eta_2^2, \eta_3^2\}$ is accordingly obtained as a function of the pair $\{\theta_2, \theta_3\}$, while the

velocity variations of the three TIMs are computed from Eqs. (19)–(21) as

$$\Delta v_1 = |\eta_1 - 1| \sqrt{\frac{\mu}{p_0}} \quad (48)$$

$$\Delta v_2 = |\eta_2 - 1| \sqrt{\frac{\mu}{p_0}} \sqrt{\eta_1^2 + 2 \left(\frac{1}{\eta_1^2} - 1 \right) (1 - \cos \theta_2)} \quad (49)$$

$$\Delta v_3 = |\eta_3 - 1| \sqrt{\frac{\mu}{p_0}} \sqrt{\frac{2p_0}{p_f} + \frac{2(\eta_2^2 - 1)}{\eta_1^2} + \eta_2^2(\eta_1^2 - 2) + 2 \left(\frac{1}{\eta_1^2} - 1 \right) (1 - \eta_2^2) \cos \theta_2} \quad (50)$$

In the singular case when $\theta_3 = 2\pi$, from the discussion in the Appendix, it is found that a transfer exists only when the constraint of Eq. (54) is met. Also, since $e_0 = e_f = 0$, Eq. (54) reduces to $\sin(\theta_2 - \theta_3) = 0$, that is, $\theta_2 = \pi$. This implies that $\text{rank } \mathbb{F} = 1$ and, from Eq. (55)

$$b = \frac{1}{2} \left(\frac{p_0}{p_f} - 1 \right), \quad c = \frac{1}{2} \left(\frac{p_0}{p_f} - 1 \right) - a \quad (51)$$

When these expressions are substituted into Eqs. (32), the result is

$$\eta_1^2 = \frac{1}{1+a}, \quad \eta_2^2 = \frac{2(1+a)}{1+2a+p_0/p_f}, \quad \eta_3^2 = \frac{1+2a+p_0/p_f}{2p_0/p_f} \quad (52)$$

that is, each η_i is function of the single variable a . The total velocity variation in this singular case is therefore function of the independent variable a only, that is, $\Delta \tilde{v}_{\text{tot}} = \Delta \tilde{v}_{\text{tot}}(a)$, and its minimum value is easily found numerically. The optimization procedure consists in applying the grid search algorithm to the nonsingular case, compare that result with the solution obtained in the singular case and select the minimum between the two values.

For example, consider a transfer involving two circular orbits with $p_f/p_0 = 2$, that is, a transfer in which the global optimal solution corresponds to a Hohmann transfer. In this case, using the proposed grid search algorithm with $\theta_3 \neq 2\pi$ rad, the optimal solution is $\Delta \tilde{v}_{\text{tot}} \simeq 0.2845$. Such a minimum value of $\Delta \tilde{v}_{\text{tot}}$ is obtained when the polar angles $\{\theta_2, \theta_3\}$ belong to the side of the triangle sketched in Fig. 4. Indeed, using Eqs. (45)–(47), a value of $\eta_3 = 1$ is obtained along the side $\theta_2 = \pi$ rad, that is, the third impulse is not performed. When $\theta_3 = \pi$ rad, it follows that $\eta_2 = 1$, and the second impulse does not occur; finally, when $\theta_3 = \theta_2 + \pi$ rad the value of η_1 is equal to 1, and the first impulse vanishes.

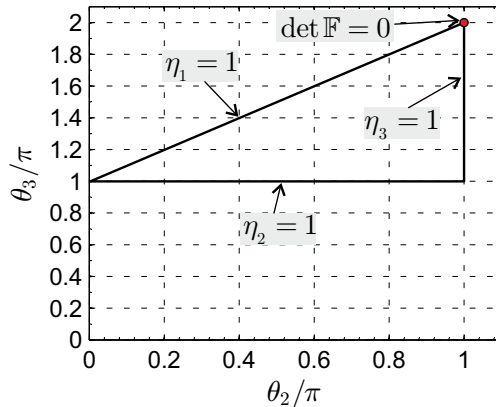


Figure 4: Contour plot of the cost function $\Delta \tilde{v}_{\text{tot}}$ for a circle-to-circle transfer with $p_f/p_0 = 2$.

Figure 5 illustrates the singular case in which $\theta_3 = 2\pi$ rad and $\Delta \tilde{v}_{\text{tot}}$ is a function of the (free) parameter a . Note that the minimum value of $\Delta \tilde{v}_{\text{tot}}$ in the singular case coincides with the value obtained when $\det \mathbb{F} \neq 0$, which is consistent with a Hohmann transfer.

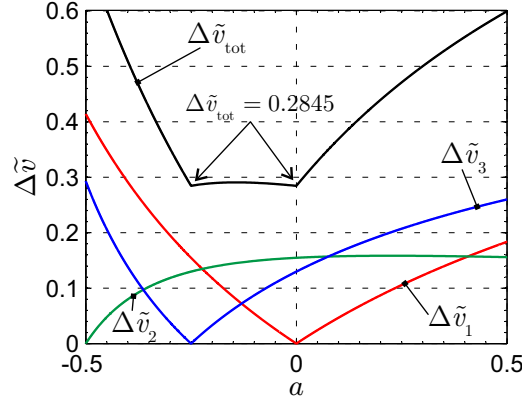


Figure 5: Singular case ($\theta_3 = 2\pi$ rad) of a circle-to-circle transfer with $p_f/p_0 = 2$.

In the case of a transfer with $p_f/p_0 = 15$, the non-singular case gives a minimum value of $\Delta\tilde{v}_{\text{tot}}$ equal to about 0.5362, which coincides with a Hohmann transfer scenario. The corresponding polar angles $\{\theta_2, \theta_3\}$ are again those reported in Fig. 4. In this case the analysis of the singular condition $\det \mathbb{F} = 0$, that is, the analysis of the function $\Delta\tilde{v}_{\text{tot}} = \Delta\tilde{v}_{\text{tot}}(a)$, gives the results reported in Fig. 6. The minimum value of $\Delta\tilde{v}_{\text{tot}}(a)$ is about 0.5212, which is obtained when $a = -0.5$. As expected, the global optimal transfer coincides with a bi-parabolic transfer in which $\theta_1 = 0$, $\theta_2 = \pi$ rad, $\theta_3 = 2\pi$ rad, and $\Delta\tilde{v}_2 = 0$.

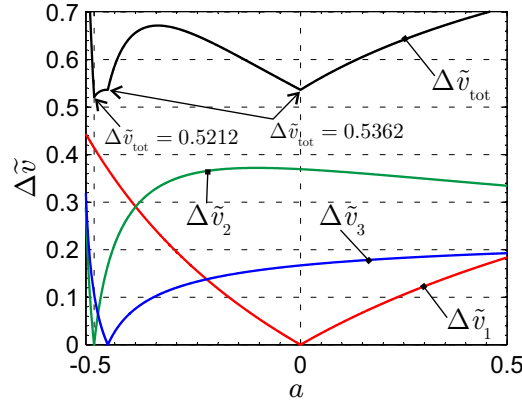


Figure 6: Singular case ($\theta_3 = 2\pi$ rad) of a circle-to-circle transfer with $p_f/p_0 = 15$.

5.2. Transfer between elliptic orbits

Consider now a transfer between two non-intersecting elliptic orbits with $p_f/p_0 = 2$, $e_0 = 0.85$, $e_f = 0.9$, and $\omega_f = 15$ deg. Using the procedure described in the previous section, and considering different values of the grid step δ , a guess of the global optimal solution was found. Table 3 shows the minimum solution obtained through the grid search procedure with different values of δ . For each δ , the whole search domain is first divided into 27 sub-domains, and the minimum solution inside each sub-domain is calculated. Using these 27 solutions as initial guesses for the local minimizer, the global minimum is chosen as the solution of the simplex method with the smallest value of $\Delta\tilde{v}_{\text{tot}}$. From the numerical simulations, a combination of grid search with $\delta = \pi/10$ rad and `fminsearch` is sufficient to locate the global minimum solution obtained with the genetic algorithm (see Tab. 1). The 27 initial guesses obtained with $\delta = \pi/10$ are shown in Tab. 4, whereas the global optimal solution found with the local minimizer requires a velocity variation of $\Delta\tilde{v}_{\text{tot}} = 0.11879996$ with $\theta_1 = 1.60434762$ rad = 91.9 deg, $\theta_2 = 3.13163856$ rad = 179.4 deg, and $\theta_3 = 8.89134554$ rad = 509.4 deg.

Note that the computational time required to run the simplex method for 27 times is about 2 s only, assuming a maximum number of 600 function evaluations from the local minimizer. It is therefore much

δ (rad)	$\Delta\tilde{v}_{\text{tot}}$	$\{\theta_1, \theta_2, \theta_3\}$ (rad)	Comp. time (s)
$\pi/10$	0.11926078	$\{1.57079633, 3.15904595, 9.145525280\}$	0.03
$\pi/20$	0.11889534	$\{1.72787596, 3.15904595, 8.988445648\}$	0.12
$\pi/45$	0.11890560	$\{1.74532925, 3.15904595, 8.970992355\}$	0.56
$\pi/90$	0.11880768	$\{1.57079633, 3.12413936, 8.866272600\}$	4.29
$\pi/180$	0.11880768	$\{1.57079633, 3.12413936, 8.866272600\}$	58.69

Table 3: Minimum $\Delta\tilde{v}_{\text{tot}}$ (and the corresponding point $\{\theta_1, \theta_2, \theta_3\}$) as a function of δ obtained with a grid search method, for the transfer with $p_f/p_0 = 2$, $e_0 = 0.85$, $e_f = 0.9$, and $\omega_f = 15$ deg. The last column shows the computational time required for the different values of the step size δ .

more efficient than the genetic algorithm, which instead requires about 300 s to run 100 times with the best combination of parameters ($N_{\text{pop}} = 100$, $N_{\text{gen}} = 20$ and $CR = 0.2$).

Point	$\Delta\tilde{v}_{\text{tot}}$	$\{\theta_1, \theta_2, \theta_3\}$ (rad)
1	0.121167586320209	$\{1.57079632679490, 2.21656815003280, 3.17649923862968\}$
2	0.132756826932681	$\{1.57079632679490, 3.15904594610974, 5.06145483078356\}$
3	0.119260776222450	$\{1.57079632679490, 3.15904594610974, 9.14552528045029\}$
4	0.120518730155416	$\{1.88495559215388, 2.21656815003280, 3.17649923862968\}$
5	0.121777770557621	$\{1.88495559215388, 3.15904594610974, 5.06145483078356\}$
6	0.119505530807041	$\{1.88495559215388, 3.15904594610974, 8.83136601509131\}$
7	0.136429295681293	$\{5.96902604182061, 7.55727566113545, 9.14552528045029\}$
8	0.134654964278445	$\{5.65486677646163, 5.98647933434055, 9.14552528045029\}$
9	0.151732100798100	$\{3.76991118430775, 5.35816080362259, 9.14552528045029\}$
10	0.123673739705876	$\{0.31415926535898, 2.21656815003280, 3.17649923862968\}$
11	0.146554126059098	$\{1.25663706143592, 3.15904594610974, 5.06145483078356\}$
12	0.120848533858465	$\{1.25663706143592, 3.15904594610974, 9.14552528045029\}$
13	0.136596156150951	$\{3.14159265358979, 6.61479786505851, 8.20304748437335\}$
14	0.131770060184756	$\{3.14159265358979, 6.61479786505851, 9.14552528045029\}$
15	0.122624531318761	$\{1.88495559215388, 3.78736447682770, 9.45968454580927\}$
16	0.123002120817665	$\{4.71238898038469, 8.18559419185340, 9.45968454580927\}$
17	0.134769790185159	$\{3.76991118430775, 5.98647933434055, 9.14552528045029\}$
18	0.136156956984973	$\{5.96902604182061, 9.44223125328932, 14.8003920569119\}$
19	0.431033684818205	$\{1.57079632679490, 7.55727566113545, 9.14552528045029\}$
20	0.134882907663829	$\{0, 5.67232006898157, 9.14552528045029\}$
21	0.135196305768108	$\{0, 5.35816080362259, 9.14552528045029\}$
22	0.120177052684727	$\{2.19911485751286, 8.18559419185340, 9.45968454580927\}$
23	0.121192441805679	$\{2.19911485751286, 7.55727566113545, 9.45968454580927\}$
24	0.125979443129990	$\{1.88495559215388, 5.67232006898157, 9.45968454580927\}$
25	0.122576694145162	$\{4.08407044966673, 8.18559419185340, 9.45968454580927\}$
26	0.138690999362560	$\{3.76991118430775, 7.55727566113545, 9.45968454580927\}$
27	0.139083851277214	$\{4.08407044966673, 9.44223125328932, 14.4862327915529\}$

Table 4: Initial guesses for the local minimizer for a transfer with $p_f/p_0 = 2$, $e_0 = 0.85$, $e_f = 0.9$, and $\omega_f = 15$ deg, obtained using a grid search method with $\delta = \pi/10$ rad.

The corresponding transfer trajectory, illustrated in Fig. 7, shows that the spacecraft completes a revolution around the primary body during the transfer, that, is, $N_{\text{rev}} = 1$. It is interesting to compare this result with the case in which the spacecraft must conclude its transfer in less than a full revolution around the primary body. Enforcing the additional constraint $N_{\text{rev}} = 0$, the proposed procedure gives a different solution, with a higher value of $\Delta\tilde{v}_{\text{tot}}$. More precisely, the optimal solution is a two-TIM transfer in which the first

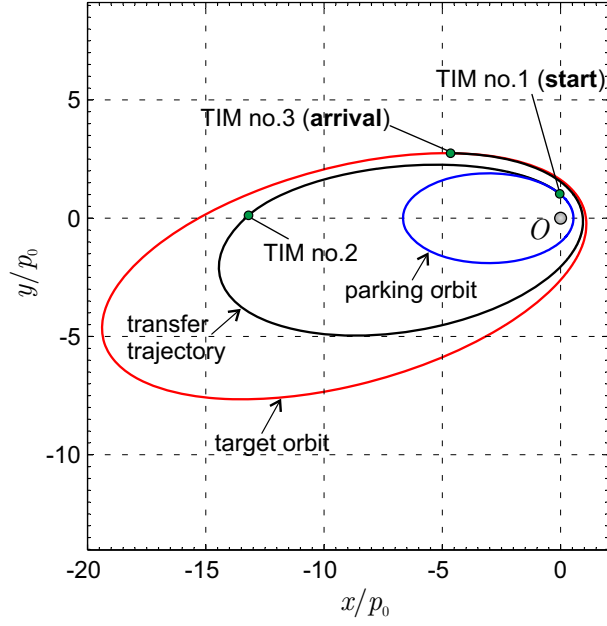


Figure 7: Optimal transfer trajectory between two ellipses with $p_f/p_0 = 2$, $e_0 = 0.85$, $e_f = 0.9$ and $\omega_f = 15$ deg.

impulse is given at $\theta_1 = 1.91863953$ rad = 109.9 deg and the second one at $\theta_2 = 3.15304641$ rad = 180.7 deg. The optimal trajectory, shown in Fig. 8, requires a $\Delta \tilde{v}_{\text{tot}} = 0.12016071$, and $\eta_3 = 1$ (the third impulse does not occur).

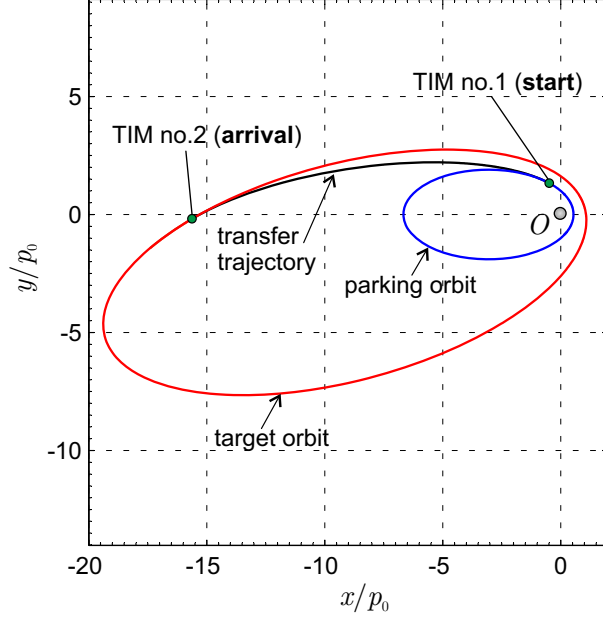


Figure 8: Optimal transfer trajectory between two ellipses with $p_f/p_0 = 2$, $e_0 = 0.85$, $e_f = 0.9$, $\omega_f = 15$ deg, and $N_{\text{rev}} = 0$.

Finally, consider a more involved case of transfer between two intersecting elliptic orbits, with $p_f/p_0 = 0.5$, $e_0 = 0.85$, $e_f = 0.9$ and $\omega_f = 20$ deg. The obtained results are reported in Tab. 5 for different values of the step size δ . For each value of δ , the search space is divided into 27 sub-domains, and the minimum solution inside each sub-domain is used as initial guess for **fminsearch**. As in the previous example, the use of a grid search with a step size $\delta = \pi/10$ rad and **fminsearch** is sufficient to find the global minimum

δ (rad)	$\Delta\tilde{v}_{\text{tot}}$	$\{\theta_1, \theta_2, \theta_3\}$ (rad)	Comp. time (s)
$\pi/10$	0.17631701	$\{2.82743339, 3.78736448, 9.773843811\}$	0.02
$\pi/20$	0.17011905	$\{2.82743339, 3.78736448, 9.930923444\}$	0.12
$\pi/45$	0.16997413	$\{2.79252680, 3.85717765, 9.878563566\}$	0.54
$\pi/90$	0.16976116	$\{2.79252680, 3.85717765, 9.913470151\}$	4.32
$\pi/180$	0.16971986	$\{2.80998009, 3.83972435, 9.896016859\}$	55.79

Table 5: Minimum $\Delta\tilde{v}_{\text{tot}}$ (and the corresponding point $\{\theta_1, \theta_2, \theta_3\}$) as a function of δ obtained with a grid search method, for the transfer with $p_f/p_0 = 0.5$, $e_0 = 0.85$, $e_f = 0.9$, and $\omega_f = 20$ deg. The last column shows the computational time required for the different values of the step size δ .

solution. The minimum velocity variation after a refinement with the simplex method is $\Delta\tilde{v}_{\text{tot}} = 0.16970489$, and the impulsive maneuvers take place at $\theta_1 = 2.80778763$ rad = 160.9 deg, $\theta_2 = 3.83928392$ rad = 220 deg, and $\theta_3 = 9.90228810$ rad = 567.4 deg. The corresponding transfer trajectory is shown in Fig. 9. The optimal transfer requires $N_{\text{rev}} = 1$.

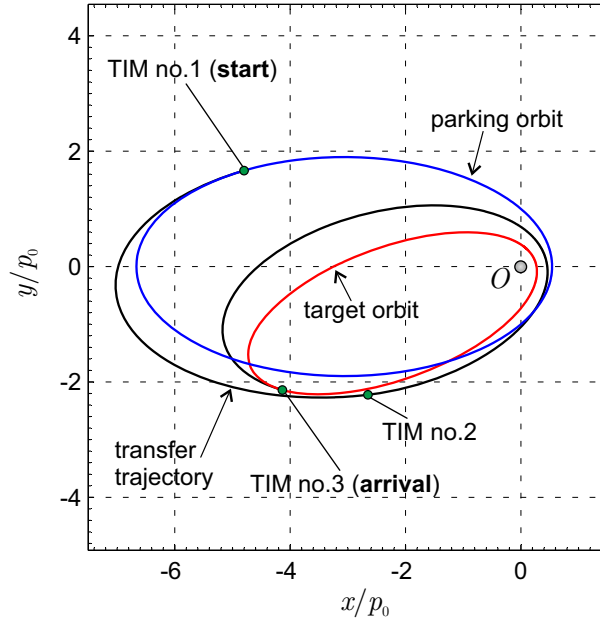


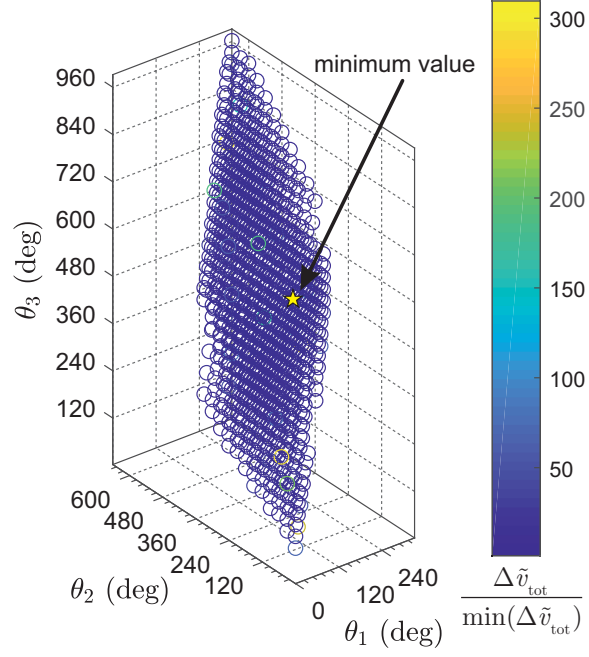
Figure 9: Optimal transfer trajectory between two intersecting ellipses with $p_f/p_0 = 0.5$, $e_0 = 0.85$, $e_f = 0.9$ and $\omega_f = 20$ deg.

A representation of the whole search domain is shown in Fig. 10 using a scatter plot, along with the position of the global optimum solution. Fig. 10(a) shows the total velocity variation as a function of the polar angles $\{\theta_1, \theta_2, \theta_3\}$, computed in a grid of points with a step $\delta = \pi/6$ rad. The points in the figure are the only feasible points (with $\eta_i^2 > 0$ and $\theta_3 - \theta_1 \neq 2\pi$ rad). Note that the vast majority of points have a value of the velocity variation close to the global minimum, even though there exist points with $\Delta\tilde{v}_{\text{tot}}$ about 300 times greater than the minimum value. To better visualize the results, Fig. 10(b) shows the points with $\Delta\tilde{v}_{\text{tot}} < 1$ only.

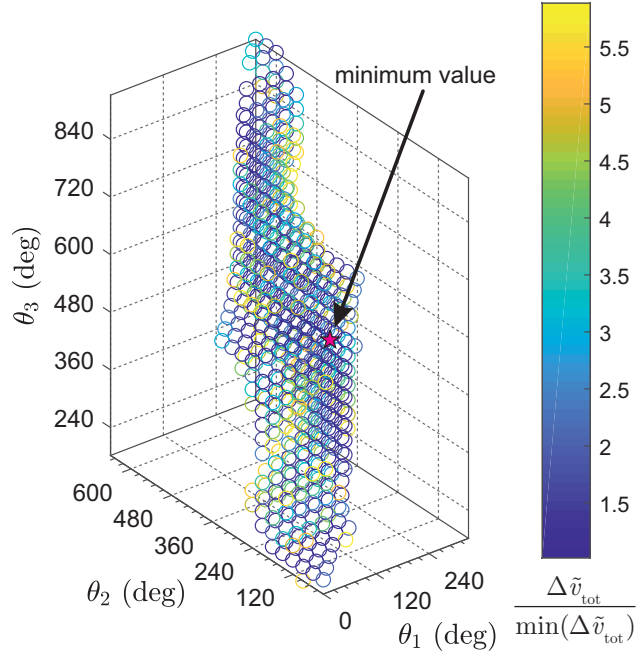
Again, when the additional constraint $N_{\text{rev}} = 0$ is enforced, the optimal transfer requires two TIMs ($\eta_3 = 1$) applied at $\theta_1 = 2.8205$ rad = 161.6 deg and $\theta_2 = 3.6924$ rad = 211.6 deg; see Fig. 11. In this case $\Delta\tilde{v}_{\text{tot}} = 0.17203389$, a value slightly greater than the global optimal value of $\Delta\tilde{v}_{\text{tot}} = 0.1697$.

Conclusions

This paper has proposed an analytical model to analyze, in terms of required total velocity variation, the two-dimensional transfer between generic elliptic orbits with a maximum number of three tangential



(a) All the grid points.



(b) Points with $\Delta \tilde{v}_{\text{tot}} < 1$.

Figure 10: $\Delta \tilde{v}_{\text{tot}} / \min(\Delta \tilde{v}_{\text{tot}})$ computed as a function of $\{\theta_1, \theta_2, \theta_3\}$, in a grid of point with step equal to $\delta = \pi/6$ rad, in a transfer scenario with $p_f/p_0 = 0.5$, $e_0 = 0.85$, $e_f = 0.9$, and $\omega_f = 20$ deg.

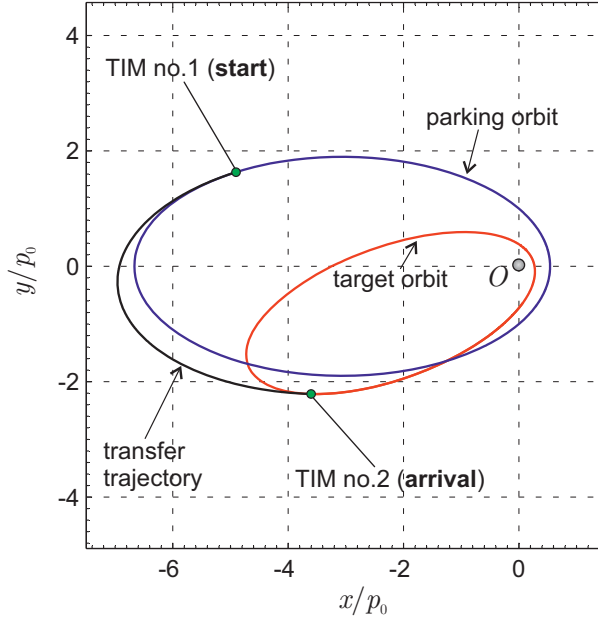


Figure 11: Optimal transfer trajectory between two intersecting ellipses with $p_f/p_0 = 0.5$, $e_0 = 0.85$, $e_f = 0.9$, $\omega_f = 20$ deg, and $N_{\text{rev}} = 0$.

impulses. The total velocity variation can be expressed as a function of the polar angles at which the three impulsive maneuvers take place. The search space is partitioned into sub-domains, and a grid search based method is used to obtain the optimal value of the performance index inside each sub-domain. The obtained solutions are then refined with a numerical method based on the simplex algorithm, which is able to find the globally optimal solution. The proposed approach has been validated with the results obtained with a genetic-based algorithm. The simulations show very similar results with the two algorithm, but the new method turns out to be much more efficient in terms of computational effort.

The proposed approach is able to find the best control strategy also when a constraint is enforced on the maximum admissible number of complete revolutions around the primary body. In the latter case, the procedure is able to manage special cases in which one of the three impulsive maneuver vanishes, that is, when the three-impulse transfer reduces to a two-impulse case.

A possible extension of this work could involve the analysis of a rendez-vous problem, by removing the constraints on the values of θ_{12} and θ_{23} to model the presence of timing and phasing requirements. In addition, the final state of the spacecraft should coincide with that of the target object along the final orbit. This problem is left to future research.

6. Appendix: Singularity of matrix \mathbb{F}

When $\theta_3 = \theta_1 + 2\pi$ rad, the determinant of \mathbb{F} in Eq. (34) is zero and the auxiliary variables a , b , and c cannot be obtained from Eqs. (37)–(39). For a thorough analysis it is necessary to distinguish according to whether $\text{rank } \mathbb{F} = 2$ or $\text{rank } \mathbb{F} = 1$.

6.1. Case of $\text{rank } \mathbb{F} = 2$

The singularity of \mathbb{F} , that is, $\theta_1 = \theta_3 - 2\pi$ implies that $\sin \theta_1 = \sin \theta_3$ and $\cos \theta_1 = \cos \theta_3$. In this case the first and third columns of \mathbb{F} are equal. As implied by the Rouché-Capelli theorem, the system (34) has a solution only if $\text{rank } [\mathbb{F}|\mathbf{w}] = 2$, that is

$$\begin{vmatrix} \sin \theta_2 & \sin \theta_3 & -e_f (p_0/p_f) \sin \omega_f \\ \cos \theta_2 & \cos \theta_3 & e_0 - e_f (p_0/p_f) \cos \omega_f \\ 1 & 1 & (p_0/p_f) - 1 \end{vmatrix} = 0 \quad (53)$$

or

$$e_f \frac{p_0}{p_f} \sin \omega_f (\cos \theta_3 - \cos \theta_2) + \left(e_0 - e_f \frac{p_0}{p_f} \cos \omega_f \right) (\sin \theta_3 - \sin \theta_2) + \left(\frac{p_0}{p_f} - 1 \right) \sin(\theta_2 - \theta_3) = 0 \quad (54)$$

Since $\{p_0, p_f, e_0, e_f, \omega_f\}$ are specified by the characteristics of the parking and final orbit, Eq. (54) has either no solution, or solutions given by isolated pairs (θ_2, θ_3) . In other terms the case $\text{rank } \mathbb{F} = 2$ gives a feasible transfer trajectory only for particular values of the triplet $\{\theta_1, \theta_2, \theta_3\}$, if any exists.

6.2. Case of $\text{rank } \mathbb{F} = 1$

The condition $\text{rank } \mathbb{F} = 1$ requires every second-order minor in \mathbb{F} to be zero. It can be easily verified that this is possible only if $\theta_1 = 0$, $\theta_2 = \pi$ rad and $\theta_3 = 2\pi$ rad. In that case, the three linear equations obtained from Eq. (34) reduce to

$$b = \frac{1}{2} \left(\frac{p_0}{p_f} - 1 - e_0 + e_f \frac{p_0}{p_f} \cos \omega_f \right), \quad c = \frac{1}{2} \left(\frac{p_0}{p_f} - 1 + e_0 - e_f \frac{p_0}{p_f} \cos \omega_f \right) - a \quad (55)$$

with the constraint

$$e_f (p_0/p_f) \sin \omega_f = 0 \quad (56)$$

The last relation implies that the condition $\text{rank } \mathbb{F} = 1$ is feasible only if $e_f = 0$ or $\omega_f = \{0, \pi\}$ rad, that is, when either the final orbit is circular, or its apse line is aligned with that of the parking orbit. In both cases b is fixed, while c depends on a free variable, since a is indeterminate; see Eqs. (55)-(56). Therefore, each η_i in Eq. (32) depends on a single variable (for example, a) and so is for $\Delta \tilde{v}_{\text{tot}}$.

References

- [1] T. N. Edelbaum, How many impulses?, *Astronautics and Aeronautics* 5 (1967) 64–69 .
- [2] F. W. Gobetz, J. R. Doll, A survey of impulsive trajectories, *AIAA Journal* 7 (5) (1969) 801–834, doi: 10.2514/3.5231.
- [3] D.-Y. Kim, B. Woo, S.-Y. Park, K.-H. Choi, Hybrid optimization for multiple-impulse reconfiguration trajectories of satellite formation flying, *Advances in Space Research* 44 (11) (2009) 1257–1269, doi: 10.1016/j.asr.2009.07.029.
- [4] Y. Wang, D. Qiao, P. Cui, Design of optimal impulse transfers from the sun-earth libration point to asteroid, *Advances in Space Research* 56 (1) (2015) 176–186, doi: 10.1016/j.asr.2015.03.040.
- [5] J. Li, Revisiting the fuel-optimal four-impulse rendezvous problem near circular orbits, *Advances in Space Research* 60 (10) (2017) 2181–2194, doi: 10.1016/j.asr.2017.08.035.
- [6] C. Xie, G. Zhang, Y. Zhang, H. Li, Optimal two-impulse rendezvous with terminal tangent burn considering the trajectory constraints, *Advances in Space Research* 54 (4) (2014) 734–743, doi: 10.1016/j.asr.2014.04.028.
- [7] Z. Zhu, Y. Yan, Two-tangent-impulse flyby of space target from an elliptic initial orbit, *Advances in Space Research* 57 (10) (2016) 2177–2186, doi: 10.1016/j.asr.2016.02.022.
- [8] V. G. Adamyan, L. V. Adamyan, G. M. Zaimtsyan, L. T. Manandyan, Double-pulse cotangential transfers between coplanar elliptic orbits, *Journal of Applied Mathematics and Mechanics* 73 (2009) 664–672, doi: j.jappmathmech.2010.01.006.
- [9] G. Zhang, D. Zhou, D. Mortari, T. A. Henderson, Analytical study of tangent orbit and conditions for its solution existence, *Journal of Guidance, Control, and Dynamics* 35 (1) (2012) 186–194, doi: 10.2514/1.53396.
- [10] G. Zhang, X. Zhang, X. Cao, Tangent-impulse transfer from elliptic orbit to an excess velocity vector, *Chinese Journal of Aeronautics* 27 (3) (2014) 577–583, doi: 10.1016/j.cja.2014.04.006.
- [11] A. A. Quarta, G. Mengali, Simple solution to optimal cotangential transfer between coplanar elliptic orbits, *Acta Astronautica* 155 (2019) 247–254, doi: 10.1016/j.actaastro.2018.12.007.
- [12] A. A. Quarta, G. Mengali, Linear systems approach to multiple-impulse trajectory analysis via regularization, *Journal of Guidance, Control, and Dynamics* 33 (5) (2010) 1679–1683, doi: 10.2514/1.50133.
- [13] J. C. Lagarias, J. A. Reeds, M. H. Wright, P. E. Wright, Convergence properties of the nelder-mead simplex method in low dimensions, *SIAM Journal of Optimization* 9 (1) (1998) 112–147, doi: 10.1137/S1052623496303470.